AIAA SciTech
13-17 January 2014, National Harbor, Maryland
AIAA Atmospheric Flight Mechanics Conference

CrossMark
click for updates

Lower Stratospheric Deployment Testing of a Ram-Air Parafoil System

Travis D. Fields*
University of Missouri, Kansas City, MO, 64110, USA
Oleg A. Yakimenko†
Naval Postgraduate School, Monterey, CA, 93943, USA
Jeffrey C. LaCombe‡ and Eric L. Wang§
University of Nevada, Reno, Nevada, 89557, USA

Downloaded by NAVAL POSTGRADUATE SCHOOL on March 16, 2016 | http://arc.aiaa.org | DOI: 10.2514/6.2014-0193

This work continues the flight testing of ram-air parafoils from high altitude weather balloons. Previous work revealed the major challenge of a zero-speed deployment from a balloon combined with the low air density environment. If the parafoil fails to inflate upon initial release at high altitude, tumbling and tangling occur almost instantaneously, thus preventing the parachute from inflating even after it descends into the lower, denser atmosphere. This paper describes further balloon flight testing of two different canopy size systems conducted to collect performance data in the rarely tested high altitude flight regime. It describes problems encountered during testing and considerations for improving the reliability of a ram-air parafoil released in a low-density zero dynamic pressure environment.

Nomenclature

a_{cent}	=	Centripetal component of payload acceleration
GS	=	Parafoil glide slope
h	=	Distance between parafoil and payload
MR	=	Mass ratio
S	=	Wetted surface area
V_A	=	Parafoil speed relative to air
V_G	=	Parafoil ground speed by GPS
V_H	=	Parafoil relative speed in horizontal direction of V_A
V_V	=	Parafoil relative speed in vertical direction of V_A
V_W	=	Atmospheric wind speed
W	=	Ratio between atmospheric wind speed and parafoil horizontal speed
α	=	Angle of attack
ρ	=	Air density
Ω	=	Spin rate

*Assistant Professor, Civil and Mechanical Engineering, 5100 Rockhill Rd, Kansas City, MO, fieldstd@umkc.edu, AIAA Member.
†Professor, Department of Systems Engineering, Code SE/Yk, oayakime@nps.edu, AIAA Associate Fellow
‡Associate Professor, Chemical and Materials Engineering, 1664 N Virginia St. MS 388, Reno, NV, lacomj@unr.edu, AIAA Member.
§Associate Professor, Mechanical Engineering, 1664 N Virginia St. MS 312, Reno, NV, elwang@unr.edu

Copyright © 2014 by the American Institute of Aeronautics and Astronautics, Inc. All rights reserved.

I. Background

This work continues experimental research on deploying ram-air parafoils in low-density zero-dynamic-pressure environment (lower stratosphere). The description of system along with potentials of using it in various applications is given by Benton and Yakimenko.[1] This parafoil systems, redesigned for a potential use as the final phase of an International Space Station sample return mission, is a derivative of a well-known system Snowflake developed for precise aerial delivery of small items from unmanned aerial assets.[2]

The 2013 series of flight tests were conducted in Nevada with two different canopy sizes: 0.93 m^2 (10 ft^2) and 3.7 m^2 (40 ft^2), with payload masses ranging from 22 to 54 N (5 to 12 lbs). It is known that many unsteady parachute phenomena, including inflation and brake release depend on the so-called mass ratio, representing the ratio of payload mass to an air mass associated with the canopy.

$$MR = \frac{M_{payload}}{\rho S^{1.5}} \tag{1}$$

If the parachute is deployed in troposphere then having MR greater than one typically results in few adverse instabilities. However, for the stratosphere drops this rule of thumb does not appear to hold true due to low air density. For simplicity, a third order polynomial is fit to standard atmospheric density data (Figure 1). Using this data in conjunction with Eq. 1, the mass ratio for each of the three flight configurations can be estimated for an entire mission. Figure 2 shows the mass ratio for two systems tested and even though they are much larger than one several dynamic instabilities occurred. Data from this paper suggests that for stratospheric drops from a balloon, the higher the MR, the more unstable the system becomes. Among all tested configurations, the small canopy/high-weight system exhibited the most unstable dynamics, and tangled quickly upon balloon release for all flight tests.

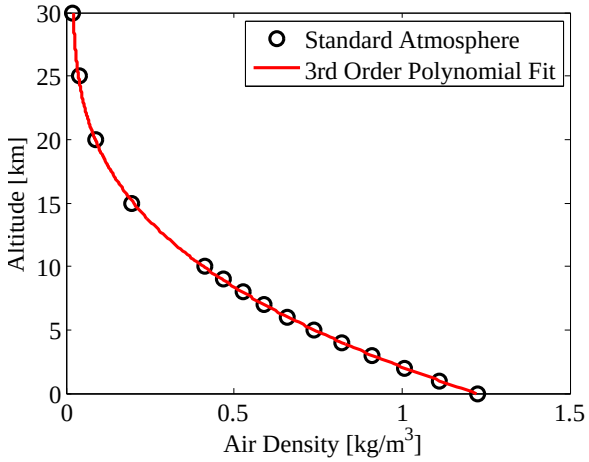

Figure 1: Polynomial fit of air density versus altitude

The 2013 test program (not fully executed) included two stages. First, flight testing was aimed at gathering data while constantly executing the same sequence of control inputs (differential flaps deflection) with a goal of investigating the effect of asymmetric brake deflection on turn rate at various altitudes. Glide slope information was also estimated by utilizing ascent collected wind information, and estimating the parafoil airspeed during descent. Later, a simple control scheme was to be used to investigate reachability sets. This scheme used a heading angle as the control parameter. A desired landing location was *preprogrammed*, with the vehicle always attempting to manipulate the GPS derived heading to match the desired heading.

This paper discusses the results of seven missions performed in the course of summer of 2013 and addresses the problems encountered as follows. Section II describes the testing methodology used for high-altitude parafoil deployments. Section III discusses testing results utilizing a simple control scheme. Section IV describes flight testing performed with only preprogrammed control inputs. Finally, section V concludes the paper with discussion, lessons learned, and recommendations for 2014 flight tests.

Downloaded by NAVAL POSTGRADUATE SCHOOL on March 16, 2016 | http://arc.aiaa.org | DOI: 10.2514/6.2014-0193

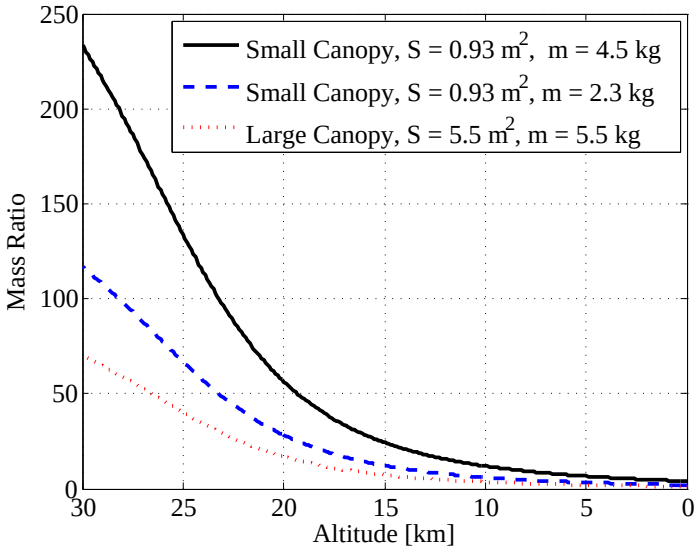

Figure 2: Mass ratio versus altitude for both small (m = 2.3 kg, & m = 4.5 kg) and large (m = 5.5 kg) canopy configurations.

II. Testing Methods

Flight testing was conducted by filling and launching a latex weather balloon. The weather balloon carries the parafoil-payload system up to the desired release altitude (approximately 30 km).

Once the balloon has been filled and tied off, the parafoil-payload is connected to the balloon. Either an electrical cutdown circuit is used at a predetermined time duration to cut the parafoil system from the balloon, or the parafoil simply begins the descent stage upon balloon burst. Figure 3 shows the small canopy system being prepped for launch. The semi-rigid canopy support frame, needed to assist in canopy inflation upon release from a balloon, can be readily seen on the upper side of the canopy. The support frame was made out of strips of spring steel. The small and large canopy systems can be seen in Figure 4, where the small canopy is on the left and the large canopy is on the right.

Figure 3: Smaller canopy being prepped for launch on high-altitude weather balloon.

The current flight testing agenda spans over two years (2013 - 2014), in order to provide sufficient data for analyzing the potential use of deploying parafoils from high altitudes. Table 1 provides the basic outline

Downloaded by NAVAL POSTGRADUATE SCHOOL on March 16, 2016 | http://arc.aiaa.org | DOI: 10.2514/6.2014-0193

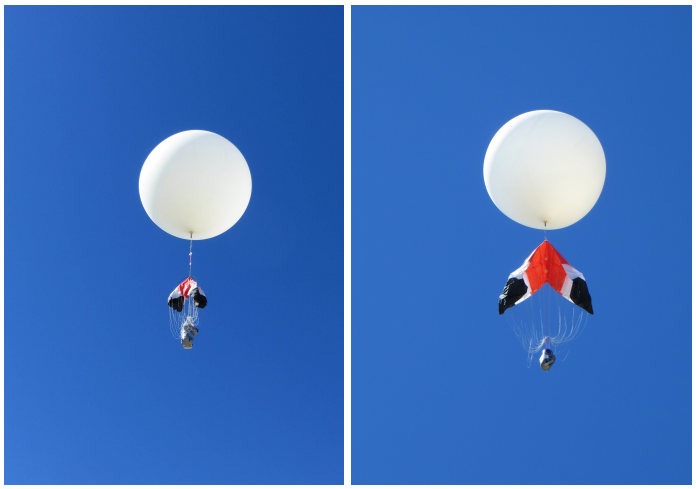

Figure 4: Small (left) and large (right) parafoil systems pictured soon after balloon release.

for the two years testing. To date seven flights have been conducted as a part of the 2013 flight testing agenda.

Table 1: 2013-2014 flight testing agenda for high-altitude parafoil testing.

Phase	Year	Flight Testing Agenda
Phase I	2013	Parachute deployment, static stability, preliminary flight maneuvers
Phase II	2014	Flight maneuvers, flight characteristics, turn rate, and glide slope

Flight testing to date (Phase 1) are considered preliminary flight testing. No major efforts were made at this point to modify control algorithms developed for low-altitude deployment as described in Ref. 2. Phase II will begin once stable deployment has been achieved in multiple drops. Nevertheless, in an effort to collect useful data from these initial flight tests, two simple control schemes were implemented. The first scheme control logic intended to steer a parafoil system towards a predetermined (preprogrammed) landing location, even if it cannot be reached due to strong winds aloft. In the nominal conditions (where have not yet been achieved) the system would attempt to manipulate the heading to match the desired heading, to reach the desired landing location. The second scheme's control logic employed a sequence of prescribed brake deflections as shown in Figure 5. This sequence was continuously repeated throughout descent to investigate the effect of asymmetric brake deflections on turn rate at various altitudes. Glide slope information was also estimated by utilizing ascent collected wind information, and estimating the parafoil airspeed during descent. Unfortunately, in the series of Phase I flight testing, issues with parafoil stability restricted the amount of useful flight characteristics data from the flight testing of both schemes. Recorded flight data consisted of onboard measurement data (accelerometer, angular rate gyro, magnetometer, altitude, latitude, longitude, pressure, and temperature), as well as both upwards and side facing video cameras.

III. Initial Flight Testing Results

As mentioned in the previous section, the initial initial flight testing involved closing the control loop with simple control logic in order to collect data. This section describes the simple control scheme, in which the vehicle attempts to navigate towards a target landing location. Navigation was determined from the GPS derived vehicle bearing. Conceptually, if the vehicle was traveling towards the target landing location, no turning input was needed; however, if the vehicle was traveling any other direction, a turning input would be applied until the vehicle direction-of-travel (regardless of vehicle orientation) matched the desired heading.

Conceptually, the control scheme attempts to control the GPS bearing by manipulating the brake deflection. For example, if the vehicle was traveling in a southerly direction and the target was easterly, the

Downloaded by NAVAL POSTGRADUATE SCHOOL on March 16, 2016 | http://arc.aiaa.org | DOI: 10.2514/6.2014-0193

Downloaded by NAVAL POSTGRADUATE SCHOOL on March 16, 2016 | http://arc.aiaa.org | DOI: 10.2514/6.2014-0193

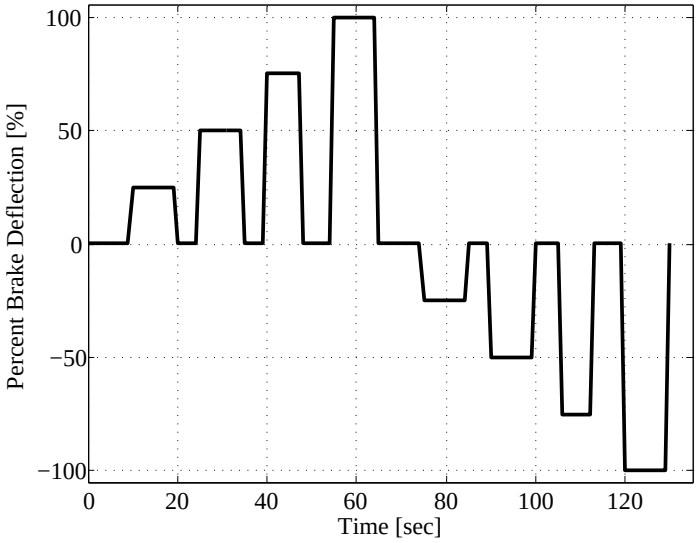

Figure 5: Schedule of turn maneuvers which were repeated during entire descent.

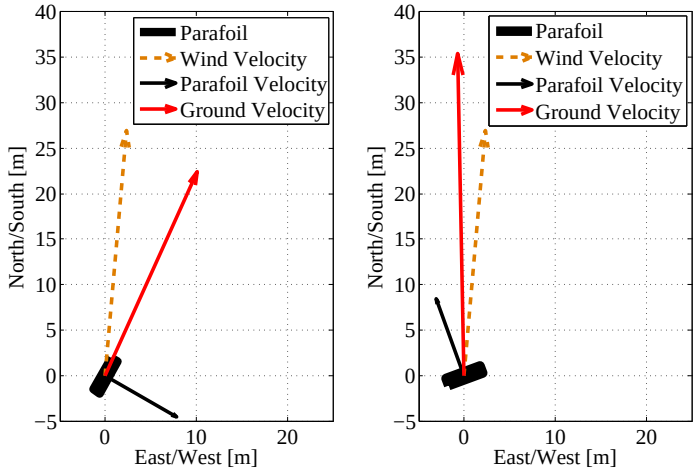

Figure 6: Top view of a parafoil with total velocity components shown for two sample parafoil directions in a high wind scenario.

control algorithm would command a left brake deflection. The turn rate was *not* controlled directly, causing the vehicle to be particularly prone to inducing a spin. Maximum safe brake deflections were determined from low altitude flight testing, and maximum programmable brake deflections were reduced further from the maximum tested deflections.

A single mission was conducted utilizing this control scheme. Total payload weight was approximately 23.3 N (5 lb) with a canopy area of 0.93 m^2 (10 ft^2). The release altitude was approximately 29.2 km (95,800 ft). Figure 7 shows the view from the payload just prior to balloon burst above northern Nevada. After balloon burst, the parafoil quickly inflated and initiated a high rate counterclockwise spin. Data was collected at 10 Hz during the entire flight. The total acceleration magnitude and yaw rate for the descent are shown in Figure 8.

It is important to notice the typically high total acceleration, particularly during the first five minutes of the descent, as the video and corresponding yaw rate data show that the payload entered into a near flat spin with rotation rates exceeding 2 Hz. The output yaw rate, as commanded by the desired brake deflection is shown below in Figure 8. The correlation between commanded turn and induced spin can be clearly seen

Figure 7: Side view of initial parafoil testing just prior to balloon burst (altitude = 29 km).

in the data during the first two thirds of descent ($\approx 29km - 10km$). The system was clearly out of control, because of the high spin rate experienced.

Videos captured during descent provided additional qualitative data showing the severe parafoil-payload flat spin during the first third of the descent phase. Figure 9 shows the extreme pitch angle of the vehicle as this camera us looking upwards toward the canopy, providing views of the horizon at the same time.

The horizontal and vertical components of airspeed can be estimated knowing the typical glide ratio of the system (when descending in a nominal regime, with no wind speed) and horizontal speed at touchdown. Assuming the vehicle is traveling at terminal velocity, the horizontal and vertical components of velocity can be derived from a simple force balance on the parafoil/payload. For this preliminary estimation, the coefficients of drag and lift are assumed to be constant over the range of flow seen during a typical flight. Although this assumption may not be valid, it permits an initial estimate of the parafoil motion at high altitudes to be determined.

Typically, the glide slope for parafoils is constant regardless of the density (although this is untested in the high altitude regime). Therefore, the relationship between the glide slope and the horizontal and vertical components of airspeed can be expressed as

$$GS = \frac{V_H}{V_V} \tag{2}$$

The overall system spin rate, denoted Ω, may have significant influence on the glide slope. Therefore, during GS estimations, only portions of the flight with small (less than $\sim$20 deg/s in spin rate) rotation rates are used. Substituting in the fact that $V_A^2 = V_H^2 + V_V^2$ into Eq. 2, V_H and V_V can be expressed in terms of glide slope, GS, and total speed directly.

$$V_H = \frac{GS\, V_A}{\sqrt{GS^2 + 1}} \tag{3}$$

$$V_V = \frac{V_A}{\sqrt{GS^2 + 1}} \tag{4}$$

Using the air density polynomial fit (Figure 1), the horizontal and vertical velocity components can be readily estimated for a range of altitudes as shown in Figure 10. For this estimate the glide slope was set to two as this is the current estimated glide slope for the Snowflake system at low altitudes. This is strictly

Downloaded by NAVAL POSTGRADUATE SCHOOL on March 16, 2016 | http://arc.aiaa.org | DOI: 10.2514/6.2014-0193

Downloaded by NAVAL POSTGRADUATE SCHOOL on March 16, 2016 | http://arc.aiaa.org | DOI: 10.2514/6.2014-0193

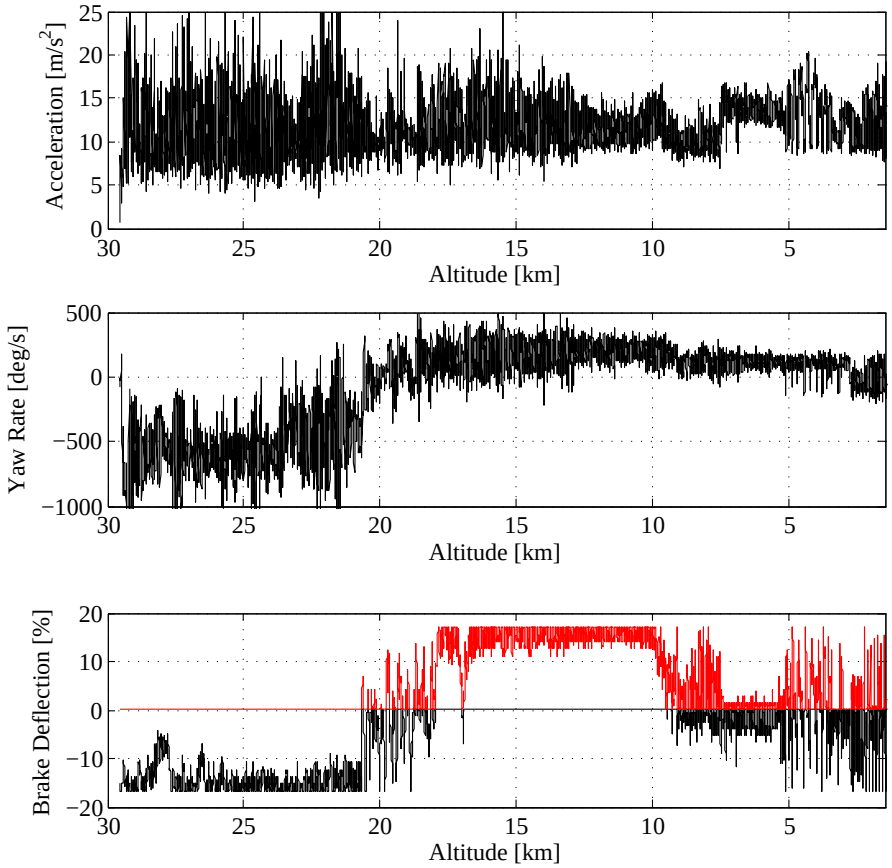

Figure 8: Total acceleration,yaw rate, and commanded brake deflection versus descent altitude. Positive brake deflection corresponds to a positive yaw rate, and negative brake deflection corresponds to a negative yaw rate.

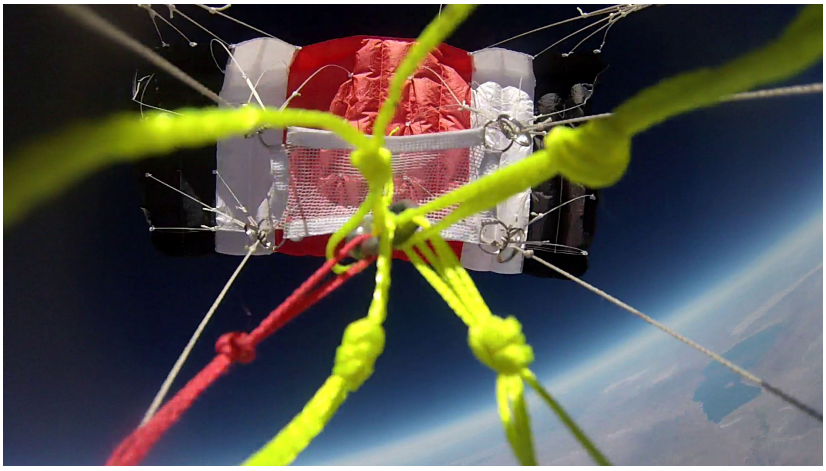

Figure 9: Upward facing camera showing near flat spin of small canopy during descent.

a theoretical estimate of the parafoil horizontal and vertical speeds. Recall that in this speed estimation the coefficients of lift and drag are assumed to be constant; thereby resulting in an estimate of the upper bound of the velocity components, as the coefficient of lift will likely decrease as density/Reynolds number decreases. If the simple control system is not successful in this best case scenario (non-changing C_D & C_L),

then it will not work for any high altitude large atmospheric wind flight scenario.

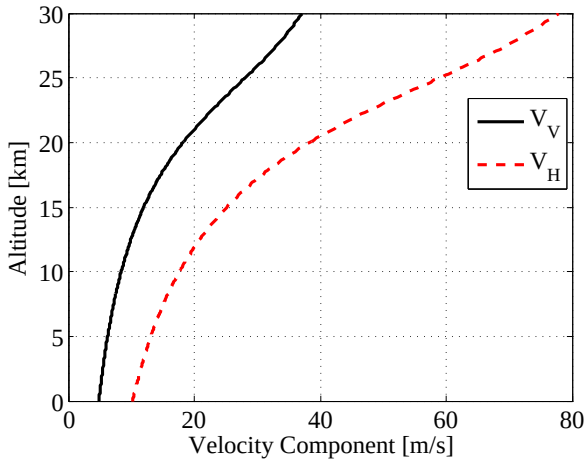

Figure 10: Parafoil velocity components versus altitude for a small parafoil canopy ($V_{H,impact} \approx 10$ m/s)

The control system attempts to control the heading, therefore, the horizontal component of the parafoil velocity (in no wind) must be significantly larger than the atmospheric wind to accurately steer the vehicle. The horizontal velocity component is compared with wind data collected from a previous balloon launch in northern Nevada in Figure 11. A ratio of atmospheric wind speed to parafoil horizontal speed is used to assist in analyzing the results. For this study, the ratio, W, is defined as:

$$W = \frac{V_W}{V_H} \tag{5}$$

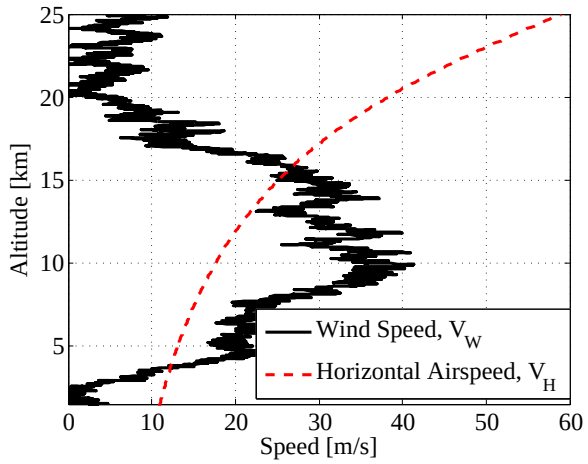

Figure 11: Parafoil horizontal speed compared with typical atmospheric wind conditions during high altitude flight testing.

For this particular flight system and wind profile simulation, the amount of time spent with $W > 1$ was 21 minutes while the time spent with $W < 1$ was 25 minutes. This shows that even with a conservative description of "high-wind scenario," the vehicle spends approximately half of the time below the high-wind cutoff of $W = 1$. Again, this is for the ideal ram-air parafoil system and the flight data collected shows significantly less horizontal speeds throughout descent. As the actual system spent much of the descent in a spin, the horizontal velocity is not accurately represented. Therefore, the actual system can not be readily compared with the idealized model.

Downloaded by NAVAL POSTGRADUATE SCHOOL on March 16, 2016 | http://arc.aiaa.org | DOI: 10.2514/6.2014-0193

IV. Prescribed Maneuver Flight Testing Results

This series of flight tests used a control logic assuming left and right brake deflections (Figure 5) thought to provide turn rate information as a function of density/altitude. Additionally, an estimate of the glide slope thought to be determined from the near zero spin rate portions of the descent. In order to calculate the glide slope, the airspeed must be estimated. This can be accomplished by estimating the wind speed from the ascent data, and subtracting the estimated wind speed from the descent speed. As the wind information for the lower altitudes is older (by the time the parafoil returns to the lower altitudes), the uncertainty in the estimated glide slope at lower altitudes will increase.

Testing was conducted with both a small 0.93 m^2 (10 ft^2) canopy and a larger 4.72 m^2 (40 ft^2) canopy. The canopies were loaded with approximately a 44.6 N (10 lb) and 53.5 N (12 lb) payload, respectively. Qualitative and quantitative data from both systems are provided in the following subsections.

A. Small Canopy Testing

Three small canopy missions have been conducted with the prescribed brake deflection maneuvers. All three of the flight tests have ended catastrophically. During ascent each canopy remained semi-inflated; due to the semi-rigid support structure on top of the canopy. As seen in Figure 12, the small canopy successfully inflates immediately after burst. For each of the three flight tests, soon after inflation the payload began to

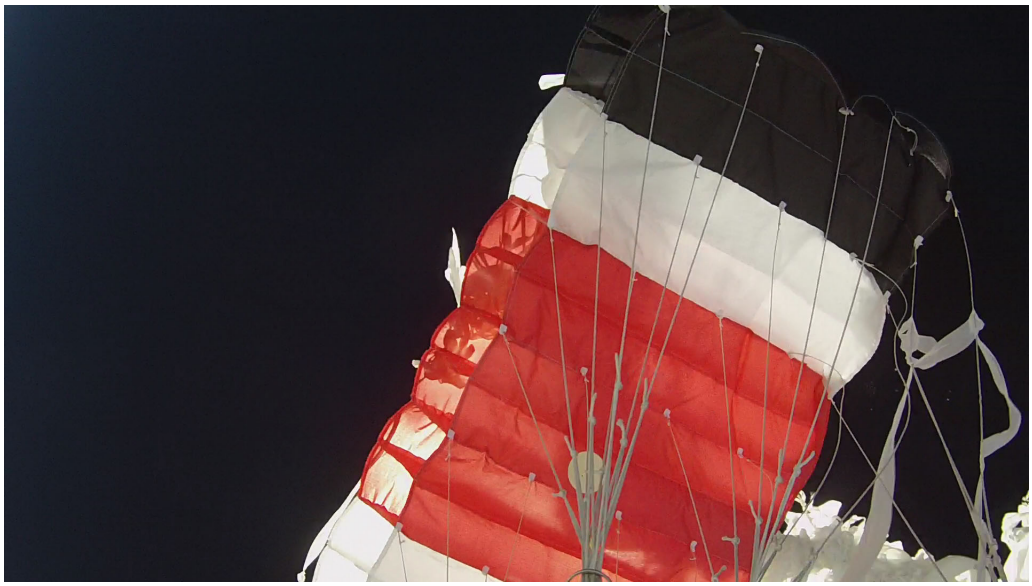

Figure 12: Upwards facing camera showing full canopy inflation after balloon burst (altitude $\approx$ 26.6 km).

rotate relative to the canopy. Figure 13 shows the collected rotation rates after release for one of the three flight tests. Within the first minute of descent, the payload spin rate increases drastically. Comparing with the video confirms that there was significant relative rotation between the payload and the canopy. Initially, the leftover balloon shards were thought to cause the problem (as can be seen in Figure 12); however, the latest experiment was performed with the use of a cutdown system (rather than ascending to balloon burst). The most recent drop test yielded the same catastrophic results, with a completely tangled/twisted canopy soon after release.

In a low density, low velocity environment (like those seen immediately after release), the canopy has a much lower dynamic pressure. The low dynamic pressure coupled with the relatively small inertia of the canopy can not provide the necessary torsional resistance through the suspension lines to maintain concentricity between the parafoil and payload orientation. Once the twisting process begins, the torsional stiffness of the suspension lines quickly decreasing (as the distance between lines quickly decreases to near zero), perpetuating the problem and removing any possibility for untwisting. Once twisted, the canopy acts essentially as a very short streamer. As the payload and canopy approach the same drag force, a flat

Downloaded by NAVAL POSTGRADUATE SCHOOL on March 16, 2016 | http://arc.aiaa.org | DOI: 10.2514/6.2014-0193

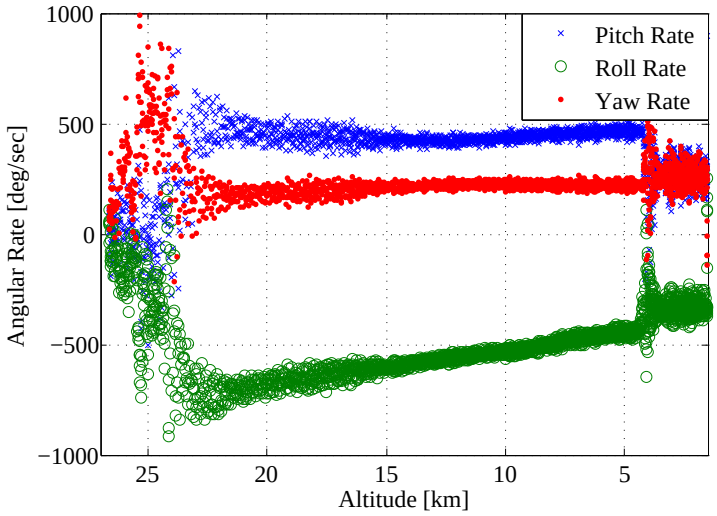

Figure 13: Measured pitch, roll, and yaw angular rates for one of the three small canopy flight tests.

spin condition occurs. An example of this flat spin is shown in Figure 14. It is important to note that the

Figure 14: Small parafoil canopy completely tangled, and spinning violently in flat spin.

very high rotation rate induced a quite large centripetal acceleration (Figure 15). The large quasi-static centripetal acceleration has a tremendous effect on the calculated orientation angles as shown in Figure 16. The rotation rates measurements show a very large rotation in all axes for most of the flight; however, the pitch and roll axes oscillate around $\sim 70°$ and $-50°$, respectively. This error is inherent in the modified complimentary filter used to estimate the system orientation. Typically, accelerometer measurements are the dominant measurement in determining orientation, with the other sensors acting as corrections during small,quick deviations. In order to successfully stabilize the canopy, software checks must be developed to counteract the influence of centripetal acceleration.

Downloaded by NAVAL POSTGRADUATE SCHOOL on March 16, 2016 | http://arc.aiaa.org | DOI: 10.2514/6.2014-0193

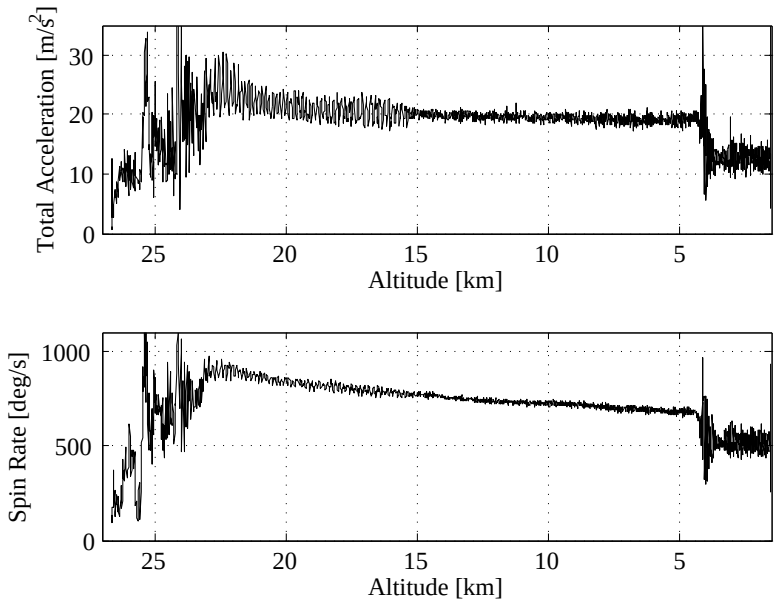

Figure 15: Spin rate and total acceleration measured during descent for the small parafoil system.

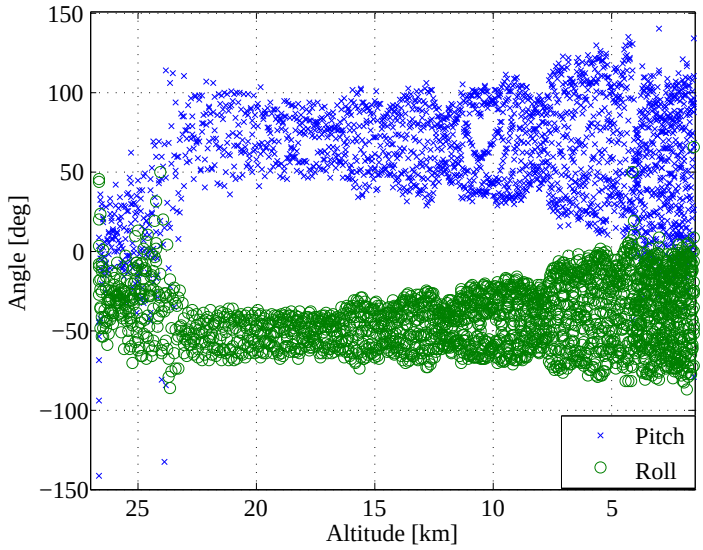

Figure 16: Calculated pitch and roll angles during descent phase.

B. Large Canopy Testing

To date, three large canopy flight tests have been performed; however, only a single flight has provided useful information (two of the three missions yielded corrupt flight log data). Therefore, results from the single complete flight log are reported, with only qualitative video data from the other two flight tests.

For all large canopy flights the canopy has inflated correctly with minimal tangling immediately following balloon burst. Similar to the small canopy, the large canopy has an umbrella system to support some of the canopy weight. This greatly improves consistency during inflation. The semi-open canopy shape can be seen during balloon burst in Figure 17. For the single quantitative flight, the control lines were tangled around the video camera during the entire descent. This can be seen in Figure 18 with the two lines converging towards

Downloaded by NAVAL POSTGRADUATE SCHOOL on March 16, 2016 | http://arc.aiaa.org | DOI: 10.2514/6.2014-0193

the camera lens. Both left and right control lines were tangled, causing a symmetric brake deflection. This limited the overall controllability of the vehicle, as well as the horizontal speed attainable.

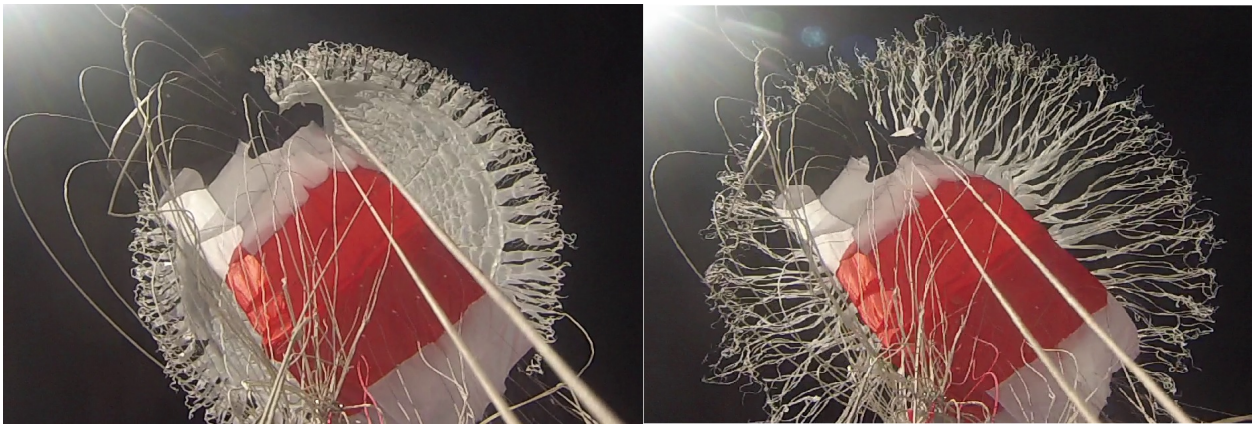

Figure 17: Canopy shown during balloon burst (Altitude = 27.8km)

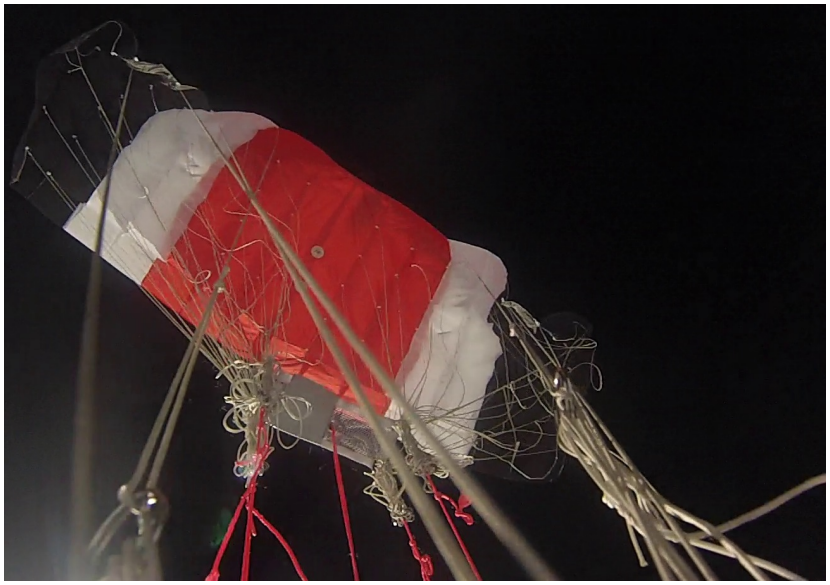

Figure 18: Large canopy fully inflated at high altitude with control lines tangled on payload.

Although controllability was reduced, the vehicle was still able to impose some brake deflection on the canopy. The collected total acceleration and yaw rate data are shown in Figure 19. From a first inspection of the spin rate data, it could be mistakenly postulated that the spin rate is higher at high altitude, and lower and low altitude; however, upon further inspection of the data, the decrease in the spin rate correlates very well with the sudden increase in total acceleration. By comparing the flight log data with the on board video data, the measured high spin rate portion of the flight corresponds well with oscillating suspension line twisting. Similar to the small canopy flight testing, the parafoil and payload have a relative rotation in the low density environment. As the large canopy has a much lower wing loading of $\approx 14N/m^2$ $(0.3lb/ft^2)$, the canopy has a sufficient restoring torque to unwind the tangled lines. Due to the low density, low damping atmosphere, the canopy-payload twisting/untwisting motion oscillates until the parafoil has reached sufficient density to dampen the motion. An example of the severity of the suspension line twisting can be seen in Figure 20.

Once the twisting motion was damped, the canopy quickly entered into a near flat spin (Figure 21). The timing of the transition from twisting to flat spin match up very closely with the increase in total acceleration. Immediately prior to the increase in acceleration, the spin rate quickly dampens out, corresponding well with

Downloaded by NAVAL POSTGRADUATE SCHOOL on March 16, 2016 | http://arc.aiaa.org | DOI: 10.2514/6.2014-0193

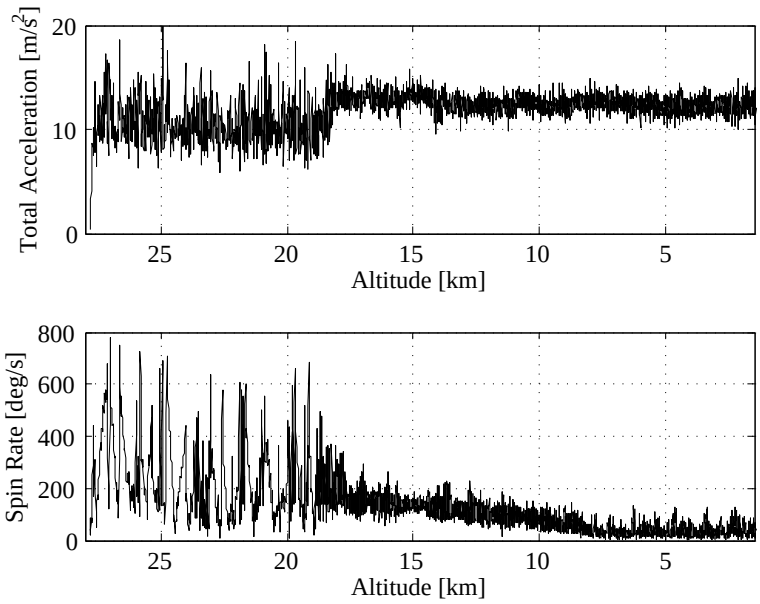

Figure 19: Spin rate and total acceleration during entire descent for the large canopy flight testing.

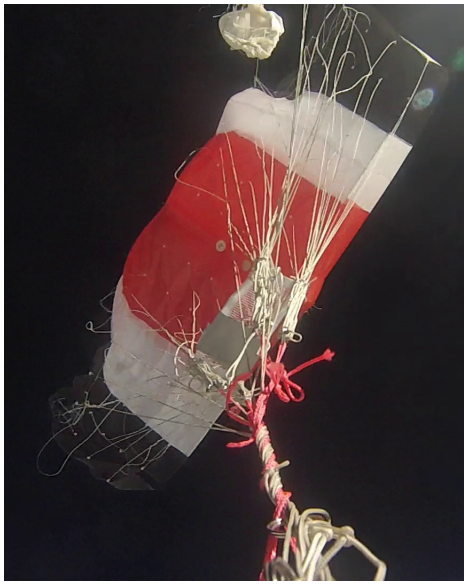

Figure 20: Canopy suspension line tangling seen throughout high altitude portion of descent.

the flight video data. The spin rate data shows a moderate, quasi-static ($\sim$ 150 deg/s) spin rate immediately after the increase in total acceleration (Figure 19). Therefore, the additional acceleration is likely a centripetal acceleration component caused from the quasi-static angular velocity. Further in the descent, the spin rate decreases to $\sim 50 deg/s$, while the total acceleration remains quasi-static. However, the onboard video shows a continuous flat spin all the way to the ground, with a rotation rate of $\sim$ 75...150 deg/s.

By assuming the primary acceleration component (aside from acceleration due to gravity) as centripetal acceleration, the corresponding rotation rate can be estimated. Centripetal acceleration has the following form:

Downloaded by NAVAL POSTGRADUATE SCHOOL on March 16, 2016 | http://arc.aiaa.org | DOI: 10.2514/6.2014-0193

Downloaded by NAVAL POSTGRADUATE SCHOOL on March 16, 2016 | http://arc.aiaa.org | DOI: 10.2514/6.2014-0193

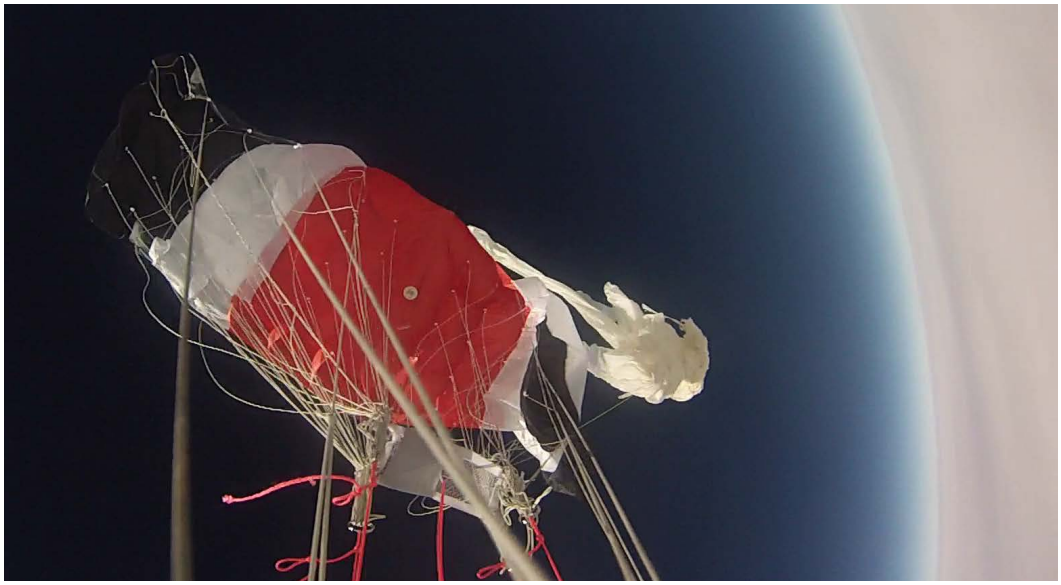

Figure 21: Snapshot showing canopy in near flat spin during descent.

$$|a_{cent}| \quad = \quad h\Omega^2 \tag{6}$$

Examining the flight data, the average acceleration (post transition) is 3.1 m/s^2. The distance between the canopy and the payload is approximately 2 m. Calculating the resulting rotation rate yields $\Omega = 71$ deg/s. It is known that rate gyro sensors are sensitive to acceleration, and it is possible the gyros could not accurately capture the rotation information in the presence of an additional constant acceleration (centripetal component). The accelerometers were capable of capturing the centripetal acceleration, with the resulting rotation rate approximately matching the onboard video data. Without the video data it may be difficult to realize the motion of the system in the presence of large rotation/accelerations on the parachute-payload system.

Additional information regarding the glide slope and dynamic pressure can be estimated from both the ascent and descent flight data. Due to the nearly constant yaw rate experienced during most of the lower altitude portion of the flight, the glide slope and dynamic pressure information have a significant uncertainty. However, the method described will work estimated these parameters in future missions. In order to estimate either the dynamic pressure or glide slope, the parafoil *airspeed* must be quantified. This presents a challenge when trying to measure the differential pressure in extremely low density environments with current commercial differential pressure systems. As an alternative, the airspeed can be estimated by comparing the wind data collected during the ascent phase of the balloon mission with the descent phase. This technique has seen use in predicting landing locations of circular parachutes with great success.[3] During ascent, the parafoil-payload are assumed to travel at the wind speed with no horizontal motion governed by the canopy. During descent, approximately the same wind is acting upon the vehicle; however, the residual speed will be the parafoil induced motion, or the airspeed. This airspeed estimation works well at high altitudes, but can have large uncertainty at low altitudes. The uncertainty increases at low altitudes because the time between ascent collected wind information and the wind experienced during descent is much larger than the time between ascent and descent phases at high altitudes. This method ignores vertical wind, as this wind is typically quite small. Using the estimated airspeed, the dynamic pressure can be estimated for the entire descent (Figure 22).

The estimated horizontal and vertical airspeeds are shown in Figure 23. The *predicted* horizontal speed (dashed line) nearly matches the estimated vertical speed for the flight test. This is due to the fact that the canopy had symmetric brake deflections and was in a spin for a significant portion of the descent. In order to reduce errors associated with high spin rates, only data with less than a 20 deg/s spin rate was used in computing the airspeed and corresponding glide slope (Figure 24). Recall that the parafoil had a constant

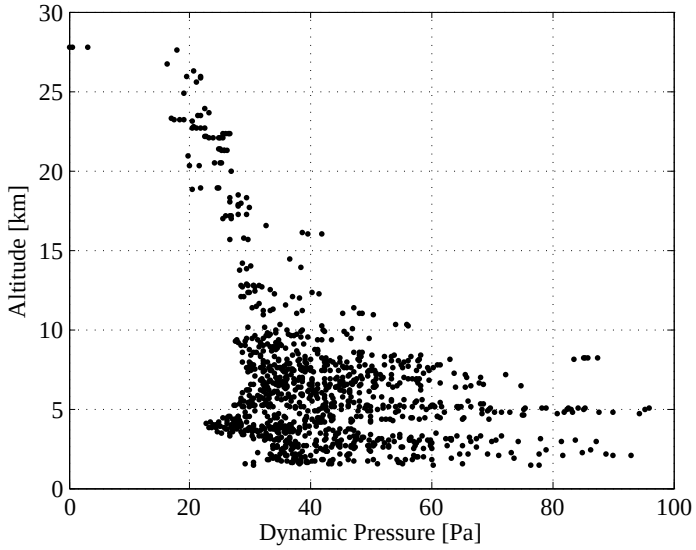

Figure 22: Estimated dynamic pressure throughout descent.

symmetric brake deflection during descent, as well as a semi-constant yaw rate (although the yaw rate was not quantified by the rate gyro sensors). These two errors have significantly effected the glide slope and speed data.

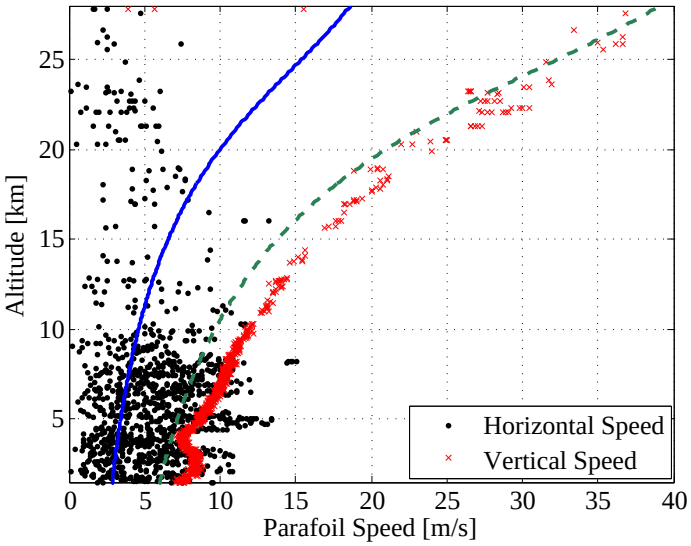

Figure 23: Estimated horizontal and vertical airspeed for large canopy flight test.

V. Conclusion and Recommendations

After performing nearly ten balloon-borne parafoil flight tests, a lingering issue with nearly all flight tests (although to varying degrees) is suspension line tangling. When deploying a parafoil canopy from rest underneath a weather balloon, the suspension lines are prone to tangling during the ascent phase. Ascent-based tangling is particularly prevalent immediately following launch, as the payload typically begins a large oscillatory motion (which is damped out during ascent). The semi-rigid frame significantly reduces the potential for suspension line tangling; however, a streamlined payload body would provide additional

Downloaded by NAVAL POSTGRADUATE SCHOOL on March 16, 2016 | http://arc.aiaa.org | DOI: 10.2514/6.2014-0193

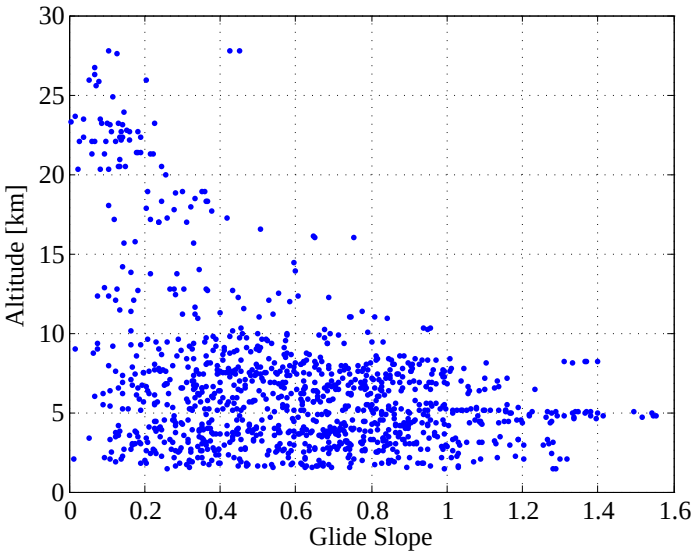

Figure 24: Estimated glide slope during entire descent. Higher uncertainty at lower altitudes is expected as wind speed is estimated from ascent wind data.

countermeasures to ascent tangling. Attention should be focused on objects protruding from the general payload shape (such as small video cameras), as these small objects tend to hook only a few lines, creating severe canopy instabilities.

Another approach to improving the suspension line tangling issue is to perform a high-speed drogue deployment of the ram-air canopy. This would eliminate suspension lines being exposed during ascent, and if performed at the necessary dynamic pressure, may remove the need for a canopy support frame. The canopy support frame proved to be quite difficult to scale (from the small to large canopy), as the larger canopy experienced significant drag during ascent. The drag attempted to close the canopy, imposing a large pressure on the canopy support frame. Even with the use of high strength carbon rods, the support frame fractured on multiple occasions (with varying degrees of severity). By simply using a drogue canopy to maintain payload stability, the parafoil could be deployed form high altitude with a large enough dynamic pressure to successfully inflate the parafoil canopy.

Finally, probably the most important issue discovered from flight testing was the consistency of the both canopies to enter a flat spin during descent. From the data, it appears the density may play a roll into the susceptibility to enter a flat spin. If the parafoil suspension lines provide sufficient damping/spring torque to minimize relative rotation between the parafoil and payload, then the vehicle will likely enter into a flat spin. This occurred with all loading ranges and canopy sizes tested. Control inputs do have some effect on the rotation rates (see Figure 8); however, the inputs may not be sufficient to completely remove the spin effects. Additionally, once the vehicle has entered the flat spin, it can be exceedingly difficult to detect the spin. As discussed previously, the flight data suggests the centripetal acceleration may have caused errors in the rate gyro sensing. By looking at the accelerometer data one can determine if the vehicle is in a constant spin; however, it can be difficult to determine the direction of the rotation from accelerometer data alone. If using attitude estimation algorithms, care must be used when calculating the current attitude, as centripetal acceleration/spins appear to greatly affect the attitude estimations.

Prior to starting Phase II, additional flight data will be collected in an attempt to further understand the spins induced after balloon release. The first step in this process is currently underway in which the payload will be significantly more streamlined, with no cameras protruding from the payload surface. Second, a relatively simple control logic will be implemented, with the sole purpose of stabilizing the canopy. In order to collect quality flight data, the canopy must be controllable and stable. The simple control scheme will attempt to minimize the spin rate data via asymmetric brake deflections. By only looking at the onboard Inertial Measurement Unit (IMU) data (and ignoring GPS derived heading), the control system should be able to stabilize the canopy. Once stable, the control system will initiate the preprogrammed control inputs

Downloaded by NAVAL POSTGRADUATE SCHOOL on March 16, 2016 | http://arc.aiaa.org | DOI: 10.2514/6.2014-0193

or tracking algorithms as originally intended.

VI. Acknowledgements

The authors would like to acknowledge the efforts of the University of Nevada, Reno BalloonSat team for launching the snowflake systems. The authors would also like to acknowledge Airborne Systems for their financial and technical support in this exploratory study.

References

[1]Benton, J. E. and Yakimenko, O. A., "On the Development of Autonomous HAHA Parafoil System for Targeted Payload Return," *Proceedings of the 22nd AIAA Aerodynamic Decelerator Systems Technology Conference and Seminar*, Daytona Beach, Florida, March 25-28, 2013.

[2]Yakimenko, O. A., Slegers, N. J., and Tiaden, R. A., "Development and Testing of the Miniature Aerial Delivery System Snowflake," *20th AIAA Aerodynamic Decelerator Systems Technology Conference and Seminar*, May 4-7, 2009, Seattle, Washington.

[3]Fields, T. D., Heninger, M. J., LaCombe, J. C., and Wang, E. L., "In-flight Landing Location Predictions using Ascent Wind Data for High Altitude Balloons," *AIAA Balloon Systems Conference*, Daytona Beach, Florida, March 26-28, 2013.

Downloaded by NAVAL POSTGRADUATE SCHOOL on March 16, 2016 | http://arc.aiaa.org | DOI: 10.2514/6.2014-0193